Supplementary Information for

Suppressor tRNAs restore functionally enhanced tumour suppressor protein to induce tumour regression

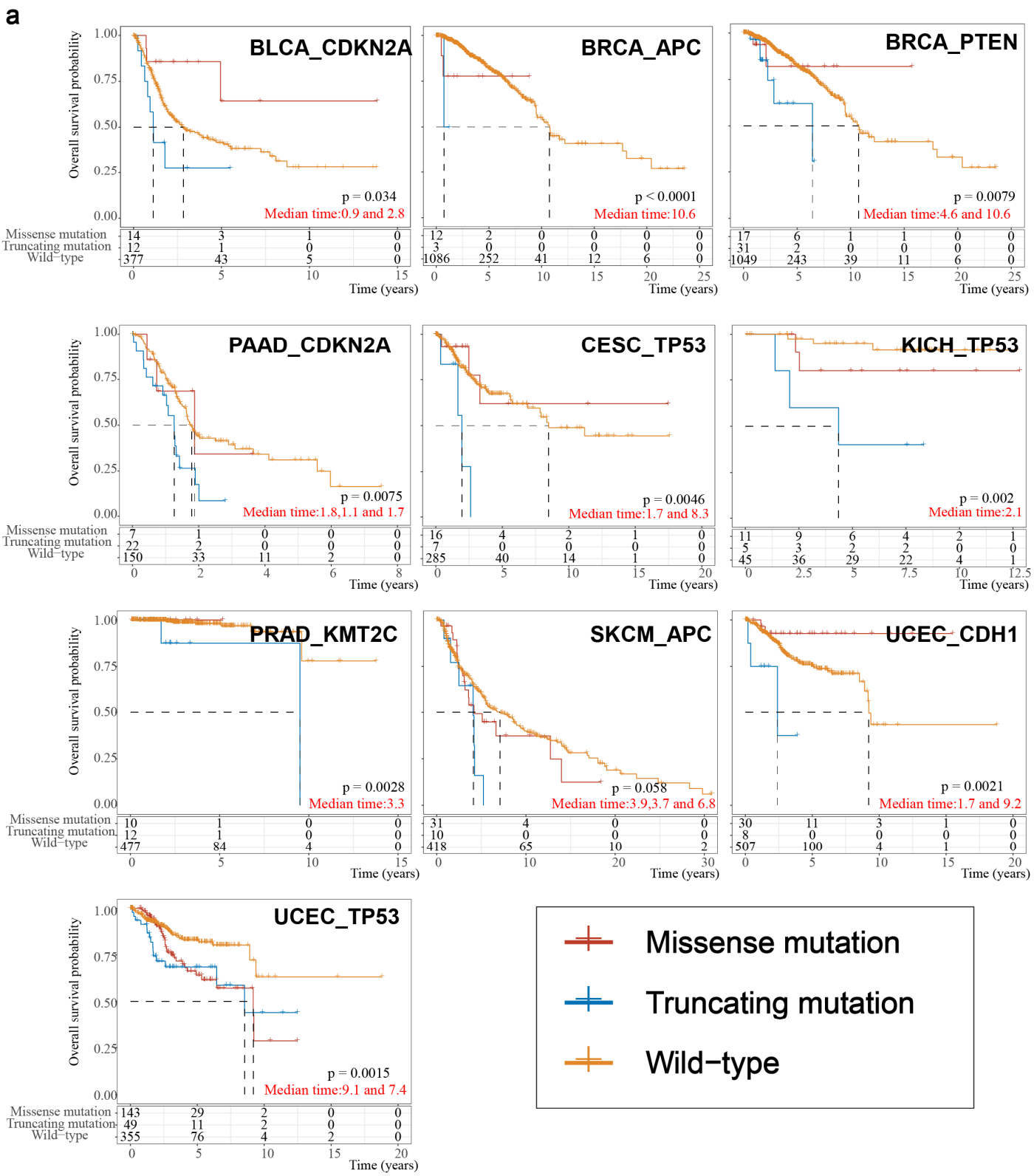
Bangyan Kong[1,2#], Zhetao Zheng[1,2#], Zeyuan Mi[1,2], Zhiyang Dou[1,2], Yuelin Yang[1,2], Yuxuan Shen[1,2], Liangzhen Dong[1,2], Jingru Lv[1,2], Ying Li[1,2], Qing Liang[1,2], Songlin Tian[1,2], Qing Xia[1,2✉]

1. State Key Laboratory of Natural and Biomimetic Drugs, Peking University, Beijing, China.

2. Department of Molecular and Cellular Pharmacology, School of Pharmaceutical Sciences, Peking University, Beijing, China.

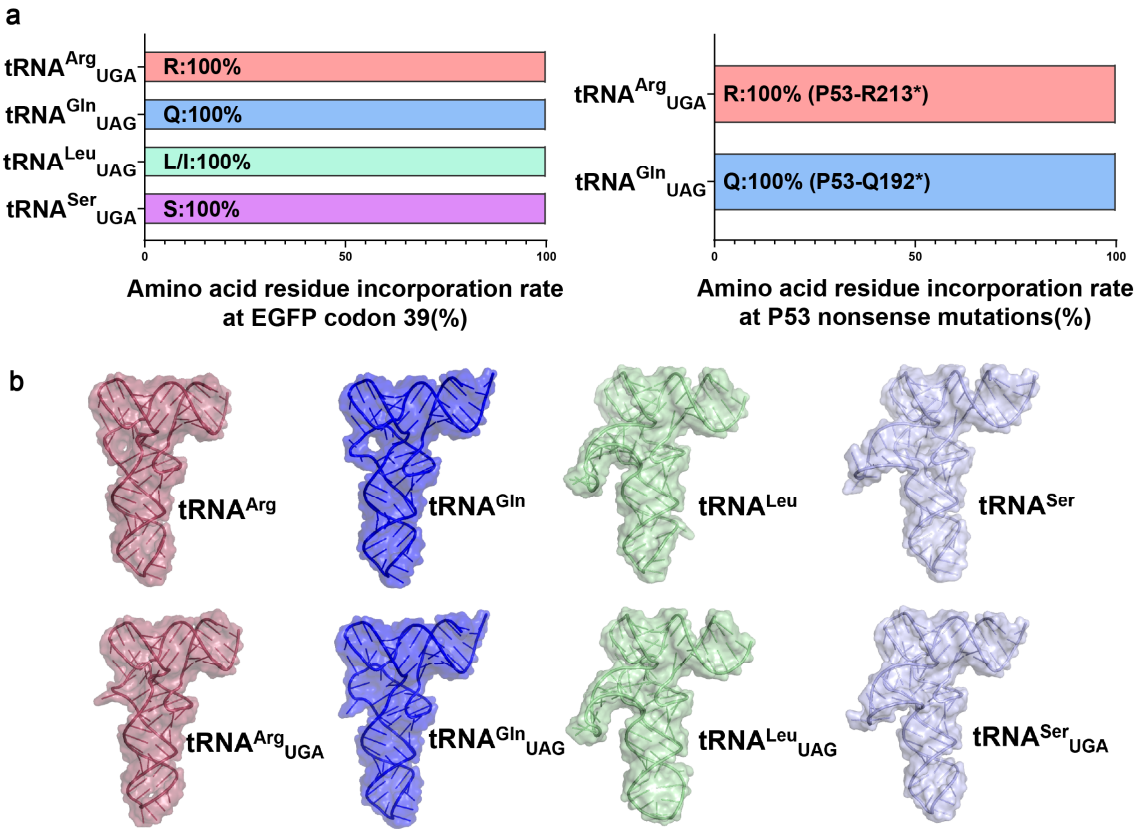
These authors contributed equally to this work.

✉ Correspondence to: xqing@hsc.pku.edu.cn



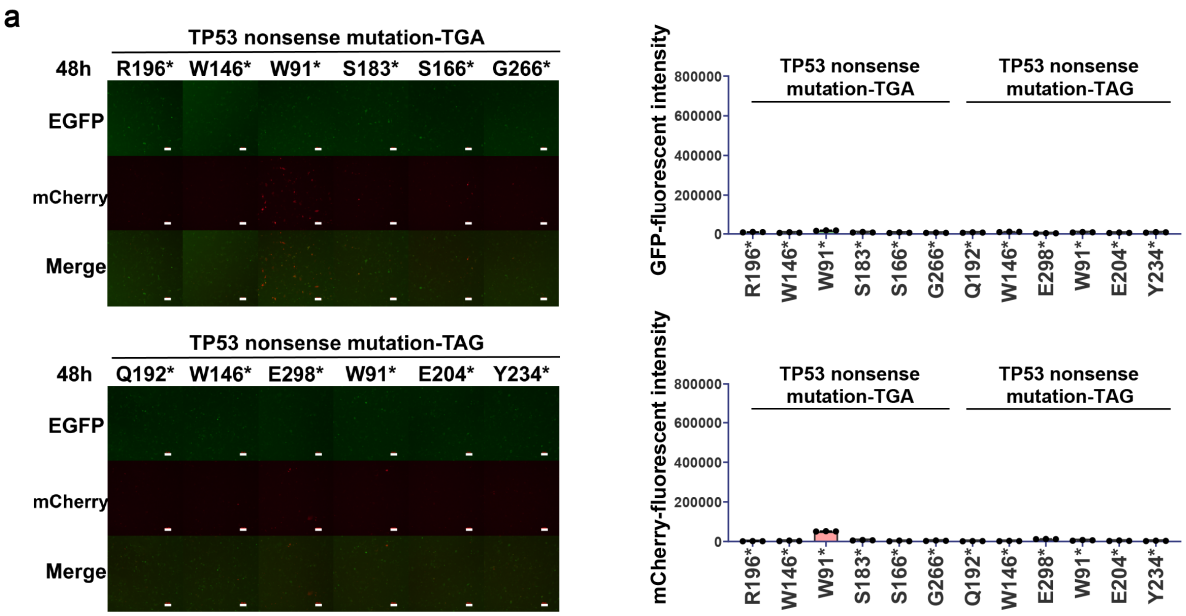
Supplementary Fig. 1 Truncating mutations in TSGs are associated with poorer prognosis in specific cancer types.

a The Kaplan–Meier survival curve distribution of different TSG mutation types groups in the TCGA dataset, with log-rank tests conducted between groups. The 95% CI represents the confidence interval for the HR. The median time represents the time corresponding to a 50% survival rate for different groups (i.e. median survival time), measured in years. The numbers in the table below represent the number of patients still in the study at a given time. The cancer types and TSGs are labeled below the picture.

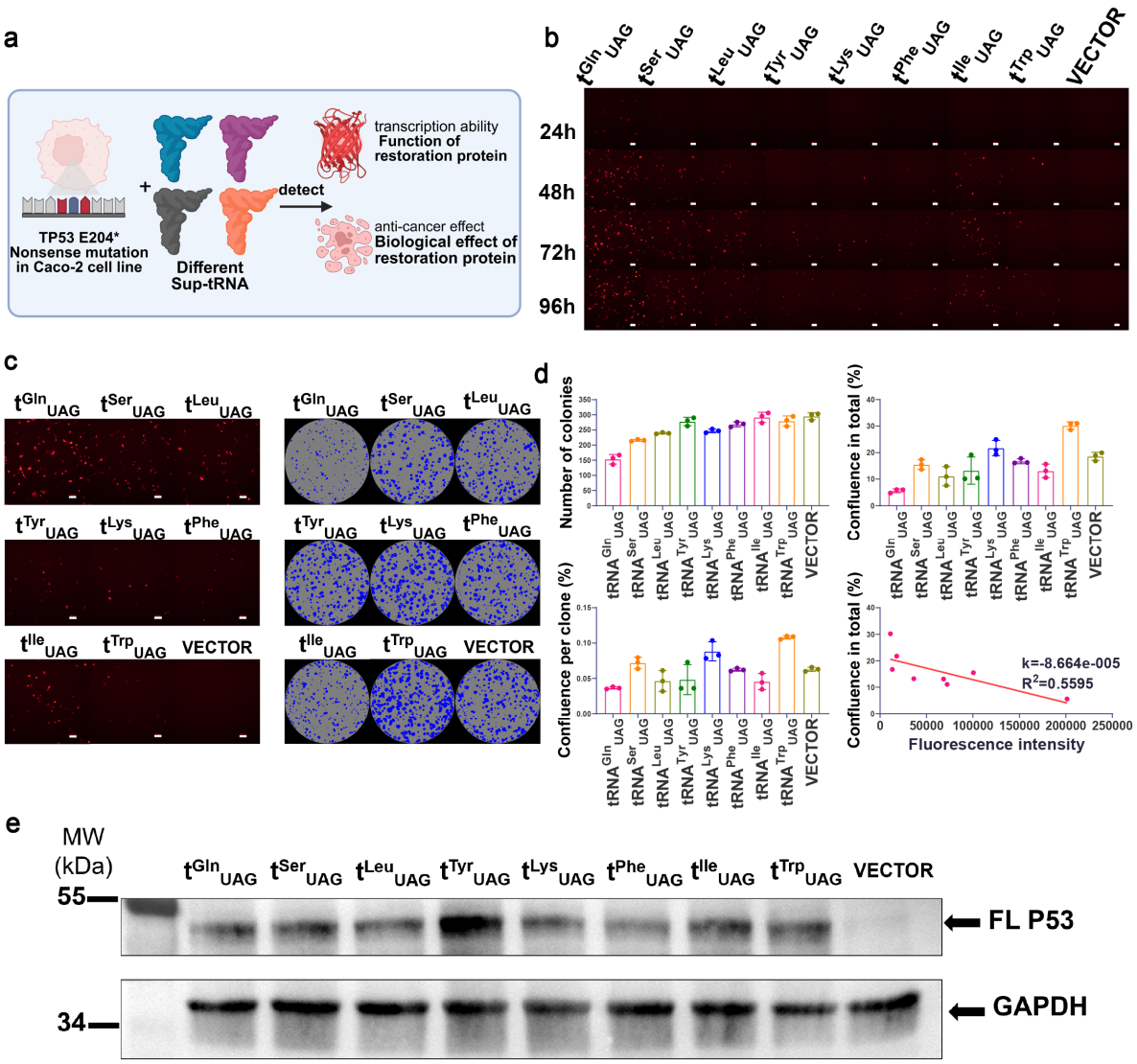


Supplementary Fig. 2 Amino acid incorporation efficiency and structural modelling of sup-tRNAs.

a Mass spectrometry analysis of amino acid incorporation rates at EGFP Y39* (left) and p*53* nonsense mutations (right) directed by various sup-tRNAs. **b** Structural models of native tRNAs and their corresponding sup-tRNA variants. Source data are provided as a Source Data file.

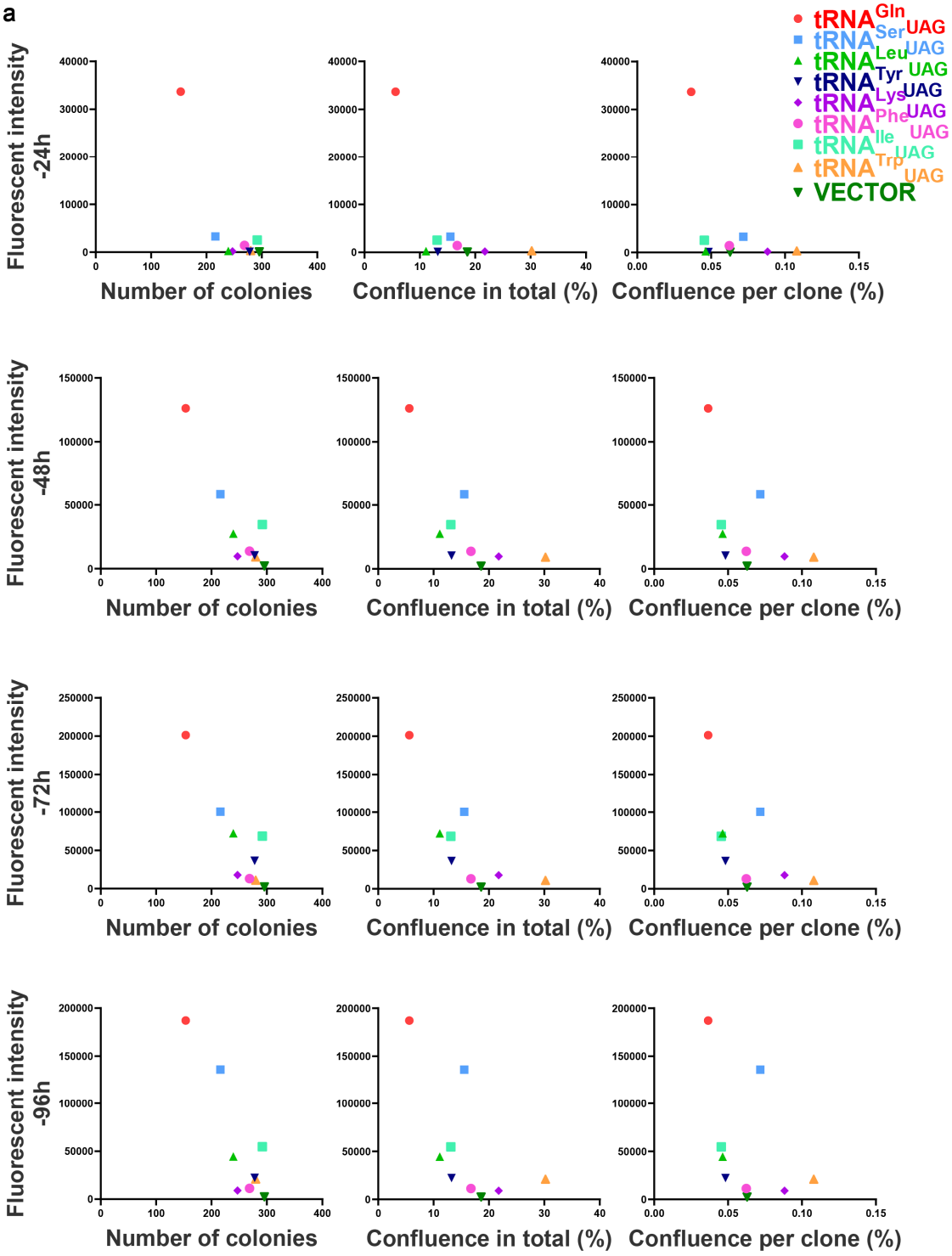


Supplementary Fig. 3 *TP53* nonsense mutations abolish p53 expression and function.
a Representative fluorescence microscopy images (left) and quantification of GFP and mCherry positive cells (right) show p53 expression and function in NCI-H1299 cells transfected with 12 different *TP53* nonsense mutants for 48 h. Data are mean ± SEM of n = 3 biological replicates. Scale bars = 100 μm. Source data are provided as a Source Data file.



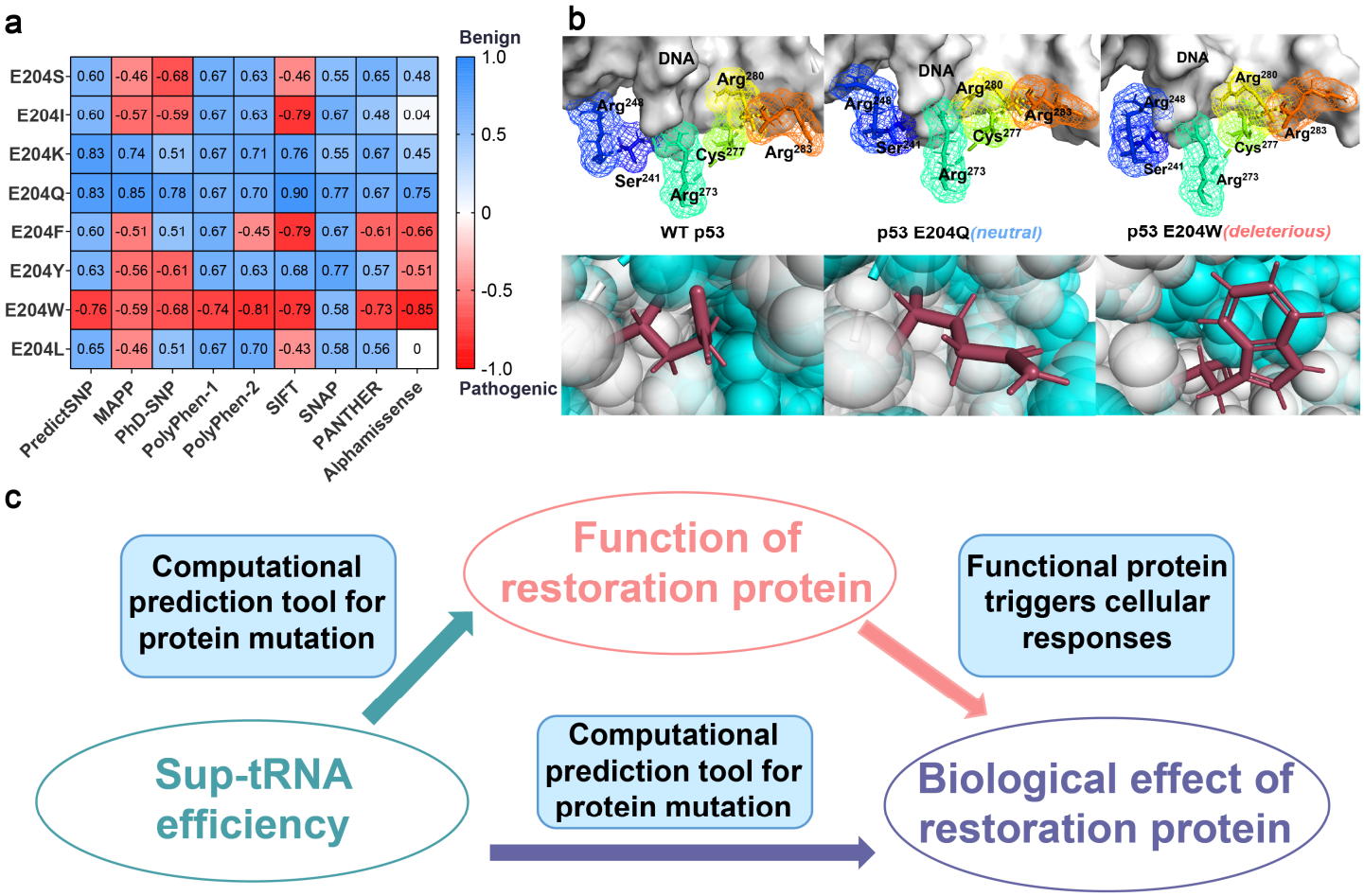
Supplementary Fig. 4 Different sup-tRNAs elicit variable antiproliferative activity through various degrees of p53 function restoration.

a Schematic of a genetically encoded reporter and colony formation system to measure p53 function and antiproliferative activity following readthrough by different sup-tRNAs. Created in BioRender. Chen, H. (2026) https://BioRender.com/5r17lr2. **b** Representative fluorescence images show various degrees of transcription function recovery of endogenous p53 in Caco-2 cells after readthrough by eight high efficiency sup tRNAs. The abbreviation of tRNA is t. Scale bar=100 μm. Data shown here were representative examples from n = 3 biological replicates. **c**, **d**, The 72h representative fluorescence images and corresponding colony formation image (**c**) & data (**d**) after readthrough by eight sup-tRNAs. Colonies are stained with crystal violet staining solution and counted after 7-10 days of culture. Scale bar = 100 μm. Colony images are acquired by Incucyte SX5 and processed and analyzed by Incucyte 2022B Rev2. Data are represented as mean ± SEM, n = 3 biological replicates. The abbreviation of tRNA is t. Ordinary least squares (OLS) linear regression was performed on the scatter points to generate the fitted trend lines presented in these plots. **e** Western blot analysis of full-length p53 recovery in Caco-2 cells after readthrough by eight sup-tRNAs. The abbreviation of tRNA is t. Data shown here were representative examples from n=3 biological replicates. Source data are provided as a Source Data file.



Supplementary Fig. 5 Sup-tRNA-induced antiproliferation activity correlates with the degree of p53 functional restoration.

a Scatter plots showing the quantitative relationship between fluorescence intensity (p53 activity) and colony formation (antiproliferative effect) at different time points after treatment with various sup-tRNAs. Data are from n=3 biological replicates. Source data are provided as a Source Data file.

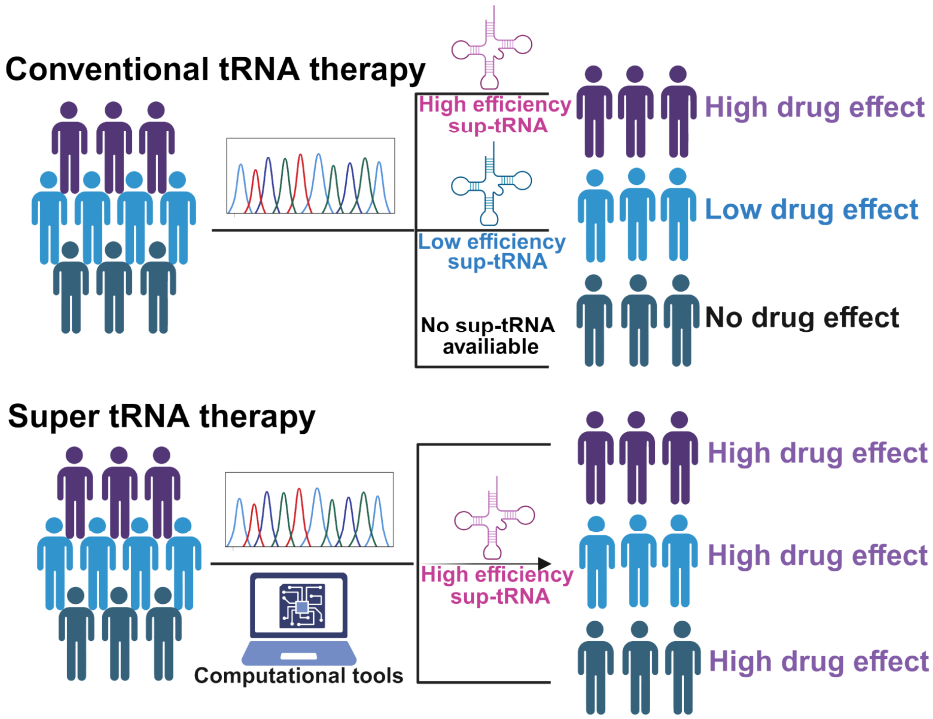


Supplementary Fig. 6 Computational prediction of neutral and deleterious mutations and the framework of the three elements of tRNA therapy.
a Predictive and functional profile of p53 E204 variants. The heat map corresponds to the predictive impact of each p53 variant ranging from -1 (Red, Pathogenic) to 1 (Blue, Benign), with the lowest score being the most deleterious. Scores from the 9 algorithms in the panels including PredictSNP, MAPP, PhD-SNP, PolyPhen-1, PolyPhen-2, SIFT, SNAP, PANTHER and Alphamissense. Red border indicates previous verified deleterious p53 variant E204W. Blue border indicates previous verified neutral p53 variant E204Q. **b** Verified deleterious and neutral p53 variants mutant site amino acid residues. The above panels show the structural models of E204Q and E204W generated from the WT p53 DBD template (PDB 2AC0). The panels below show the DNA binding peptides and DNA close-up view of the wild-type p53, neutral variant p53 E204Q and deleterious variant p53 E204W. The side chains of the six classic DNA binding residues are shown as sticks. **c** Summary of the framework among sup-tRNA readthrough efficiency, function of restoration protein and biological effect of restoration protein. Source data are provided as a Source Data file.

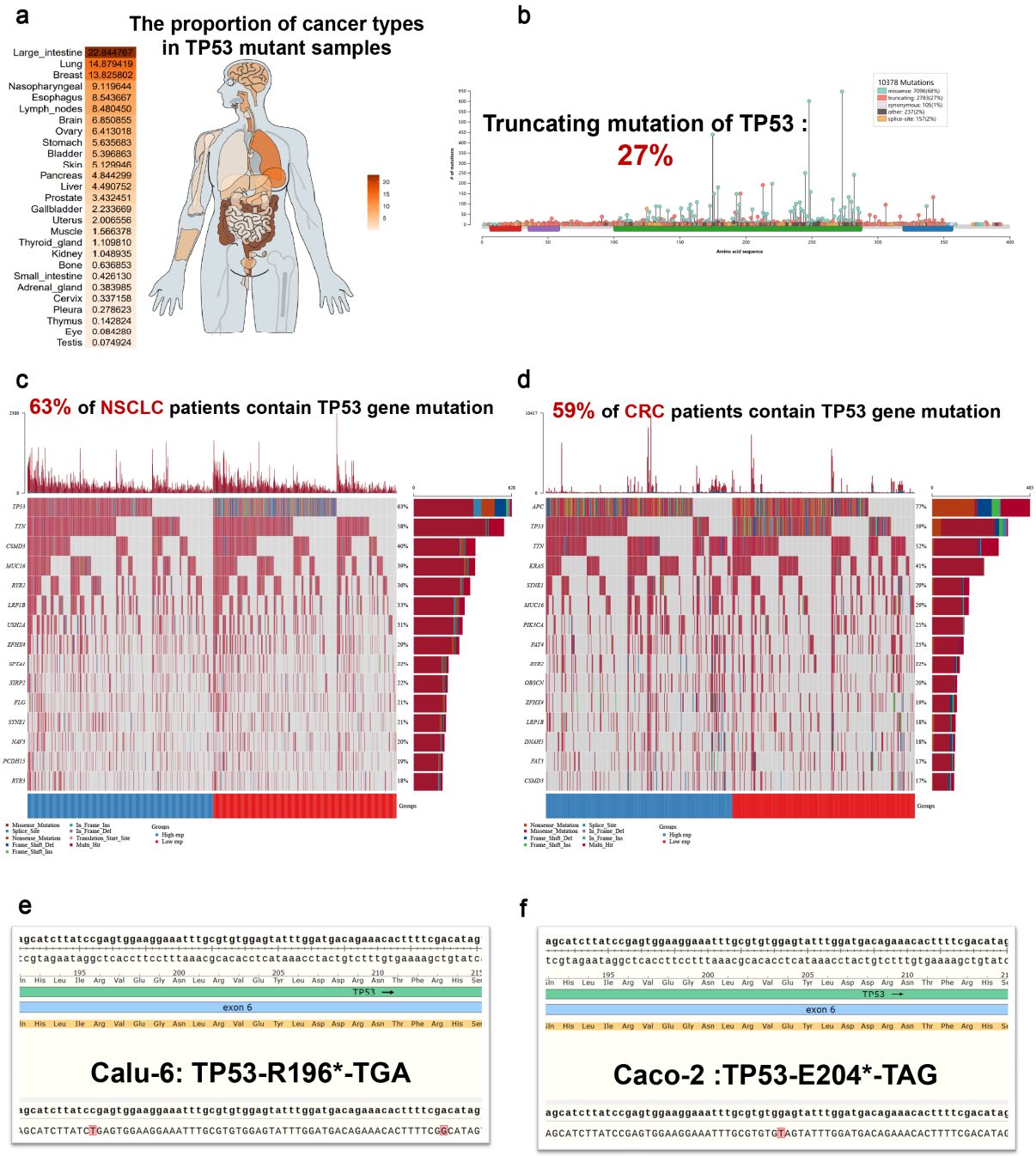
a

	A. Restore to the original amino acids?	B. Protein expression	C. Protein function	D. Biological effect
Primary-sup-tRNA	Yes	Original	Original	Original
Lower-sup-tRNA	No	Lower	Lower	Lower
Super-tRNA	No	Higher	Original	Higher
Superb-tRNA	No		Higher	Higher

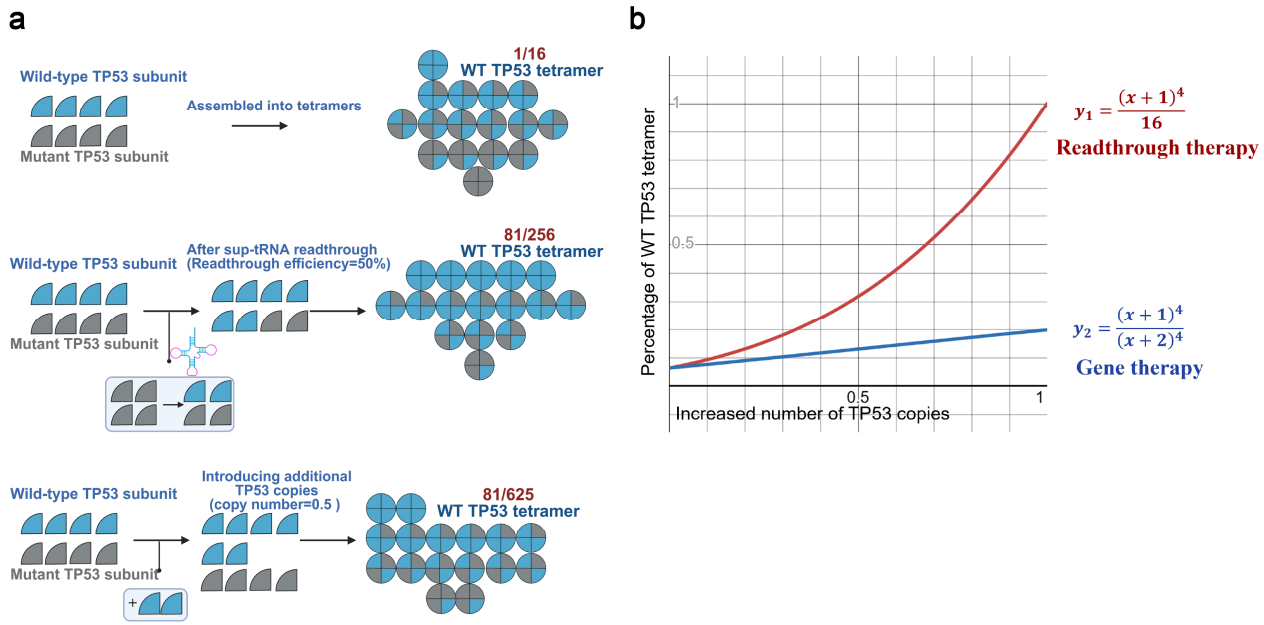
b



Supplementary Fig. 7 Definitions and classification of super-tRNA and superb-tRNA therapies.
a Classification and definitions of four sup tRNA based therapeutic strategies: primary sup-tRNA (restores wild-type variant), super-tRNA (restores neutral variant), superb-tRNA (restores advantageous variant) and lower-sup-tRNA (restores deleterious variant). **b** Comparison of conventional and super-tRNA therapy. Super-tRNA therapy expands the treatable patient population and enhances therapeutic efficacy through computationally guided selection of high efficiency sup-tRNAs that introduce neutral or advantageous amino acids. Created in BioRender. Chen, H. (2026) https://BioRender.com/118lp39.

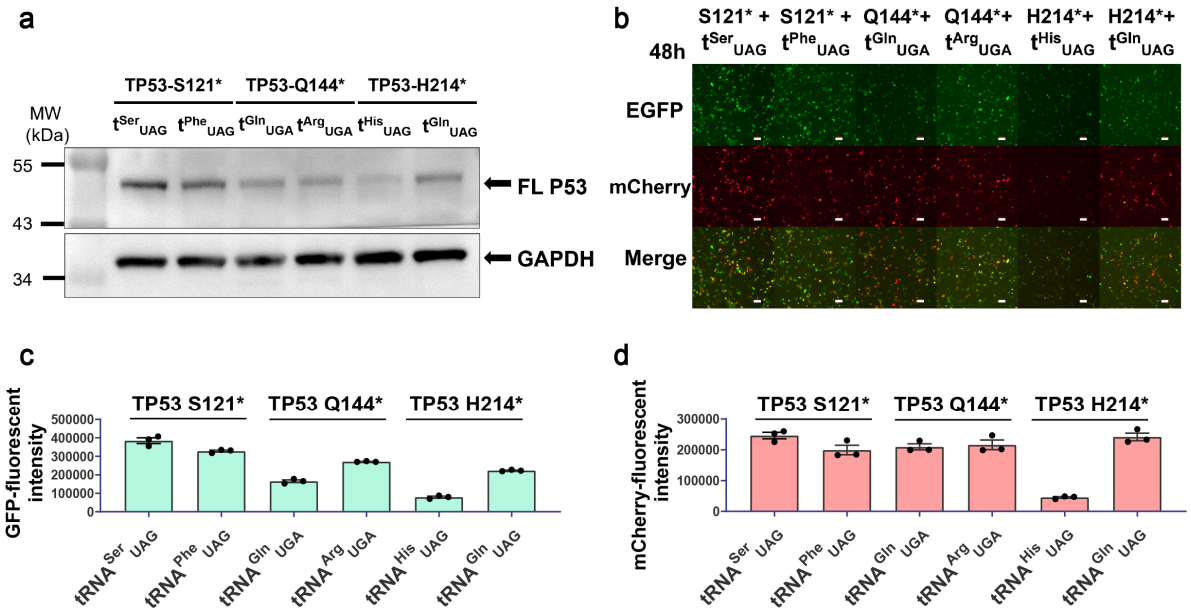


Supplementary Fig. 8 *TP53* landscape and cell lines validation.
a Cancer type distribution of *TP53* mutations. Data were downloaded from COSMIC. **b** Lollipop diagram showing the mutation distribution of the *TP53* exon gene, where the mutation type and rate are indicated by the right of the figure. The *TP53* mutation data were extracted from IntOGen. **c**, **d** Oncoplot showing the somatic mutation landscape of the NSCLC (**c**) and CRC (**d**) tumour cohort. Genes are sorted by mutation frequency and samples are sorted by disease histology, as indicated in the annotation bar at the bottom. The sidebar graph shows the types and numbers of gene mutations. The waterfall graph shows the mutation information for each gene in each sample, with different colors with specific annotations at the bottom representing different mutation types. **e**, **f** Sequencing confirmation of genomic *TP53* nonsense mutations in Calu-6 (**e**) and Caco-2 (**f**) cell lines.



Supplementary Fig. 9 tRNA therapy can better overcome the dominant negative (DN) effect than gene therapy.

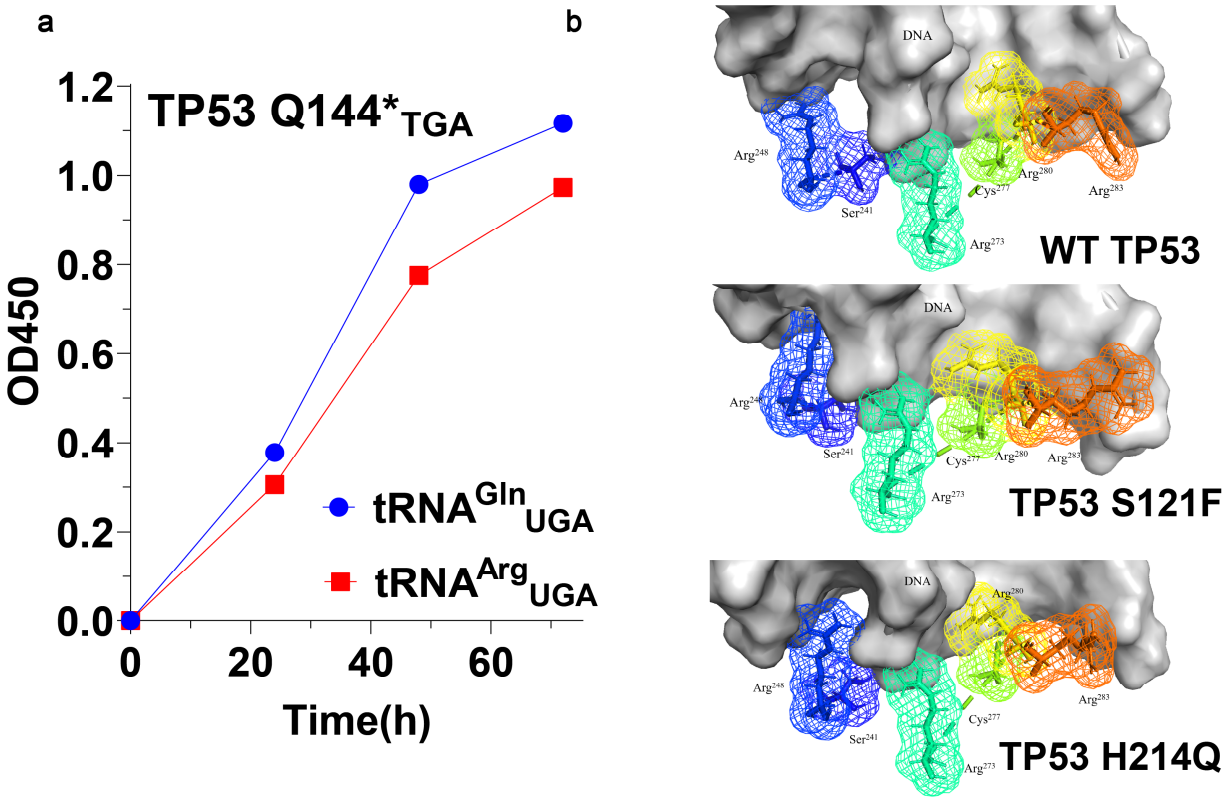
a, **b**, Workflow (**a**) and mathematical predict (**b**) about tRNA therapy can convert some of mutant p53 subunit (truncated p53 variants with an intact oligomerization domain) into wild-type p53 subunit, thereby forming more wt p53 tetramers than gene therapy. Created in BioRender. Chen, H. (2026) https://BioRender.com/ja9zx7r.



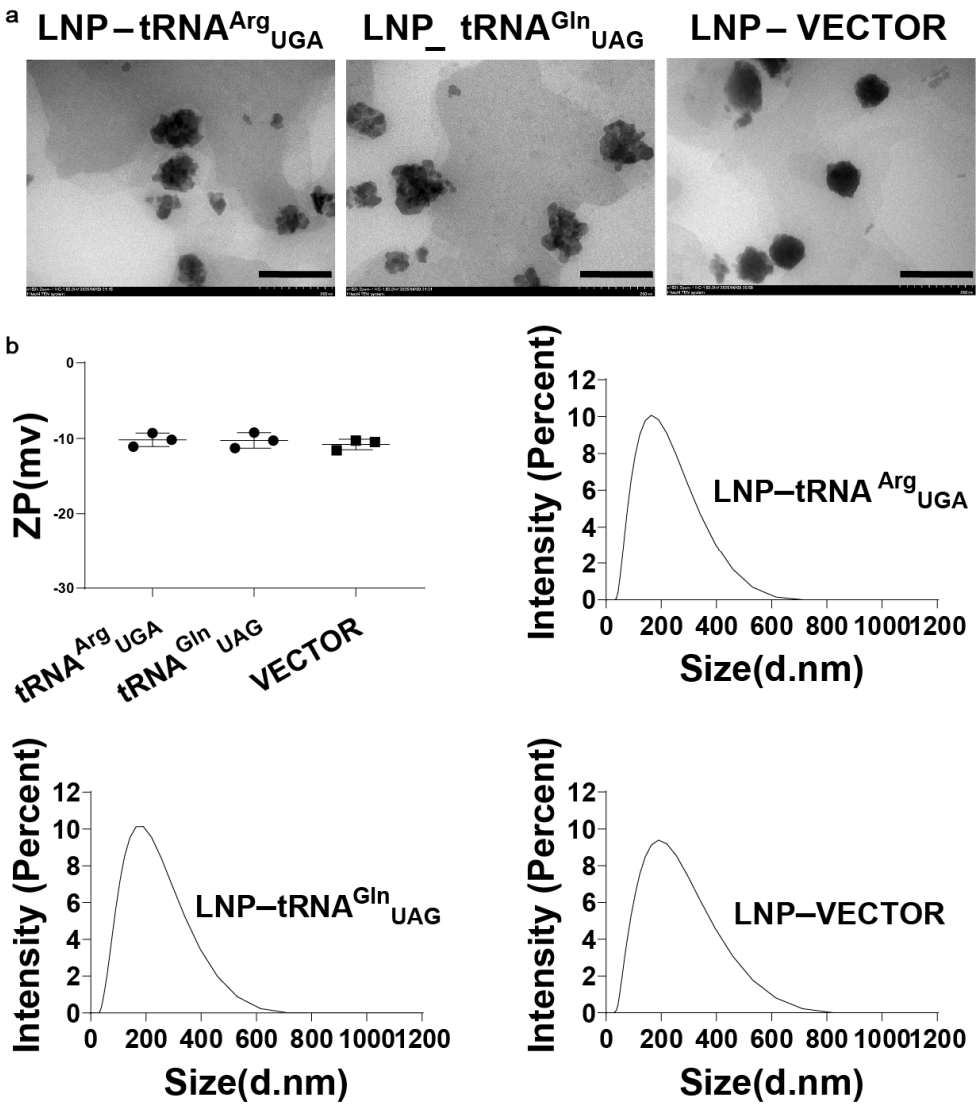
Supplementary Fig. 10 The superb-tRNA restores p53 expression and function from *TP53* S121*, Q144* and H214*.

a Western blot analysis of wild-type or enhanced p53 recovery in NCI-H1299 cells with *TP53* nonsense mutations (S121*, Q144*, H214*) after specific sup-tRNAs readthrough after 48h transfection. The abbreviation of tRNA is t. Data shown here were representative examples from n = 3 biological replicates. **b-d** Representative fluorescence microscopy images (**b**) and quantification of GFP(**c**) and mCherry(**d**) positive cells show p53 expression and transcriptional

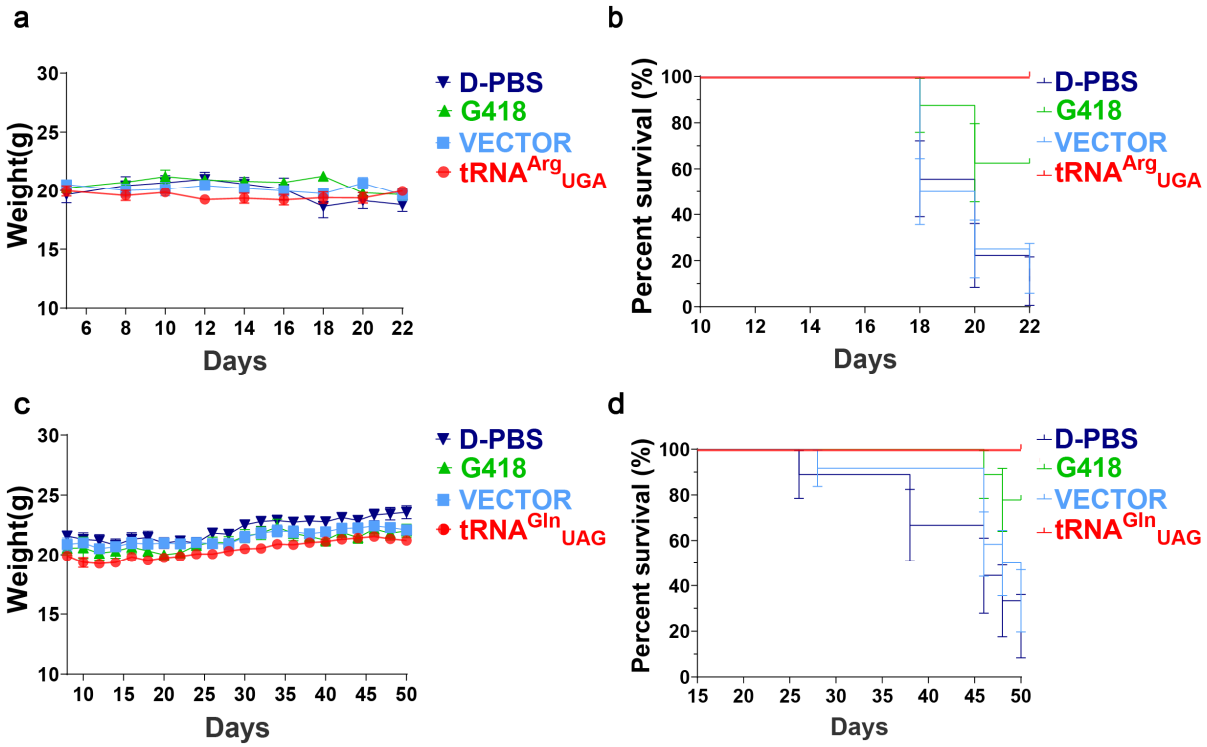
activity in NCI-H1299 cells with *TP53* nonsense mutations (S121*, Q144*, H214*) after specific sup-tRNAs readthrough after 48h transfection. The abbreviation of tRNA is t. Data are mean ± SEM of n=3 biological replicates. Scale bars = 100 μm. Source data are provided as a Source Data file.



Supplementary Fig. 11 Relative cell viability and p53 structure simulation of the superb-tRNA therapy.
a Relative cell viability measured by CCK 8 assay. After transfecting cell for 8 hours, the NCI-H1299 cells are digested, spread in plates and further measured. Data are mean ± SEM of n=3 biological replicates. **b** Close-up view of the p53 DNA binding peptides and DNA. including wild-type p53, enhance p53 variants S121F & H214Q. The side chains of the six classic DNA binding residues are shown as sticks. Source data are provided as a Source Data file.

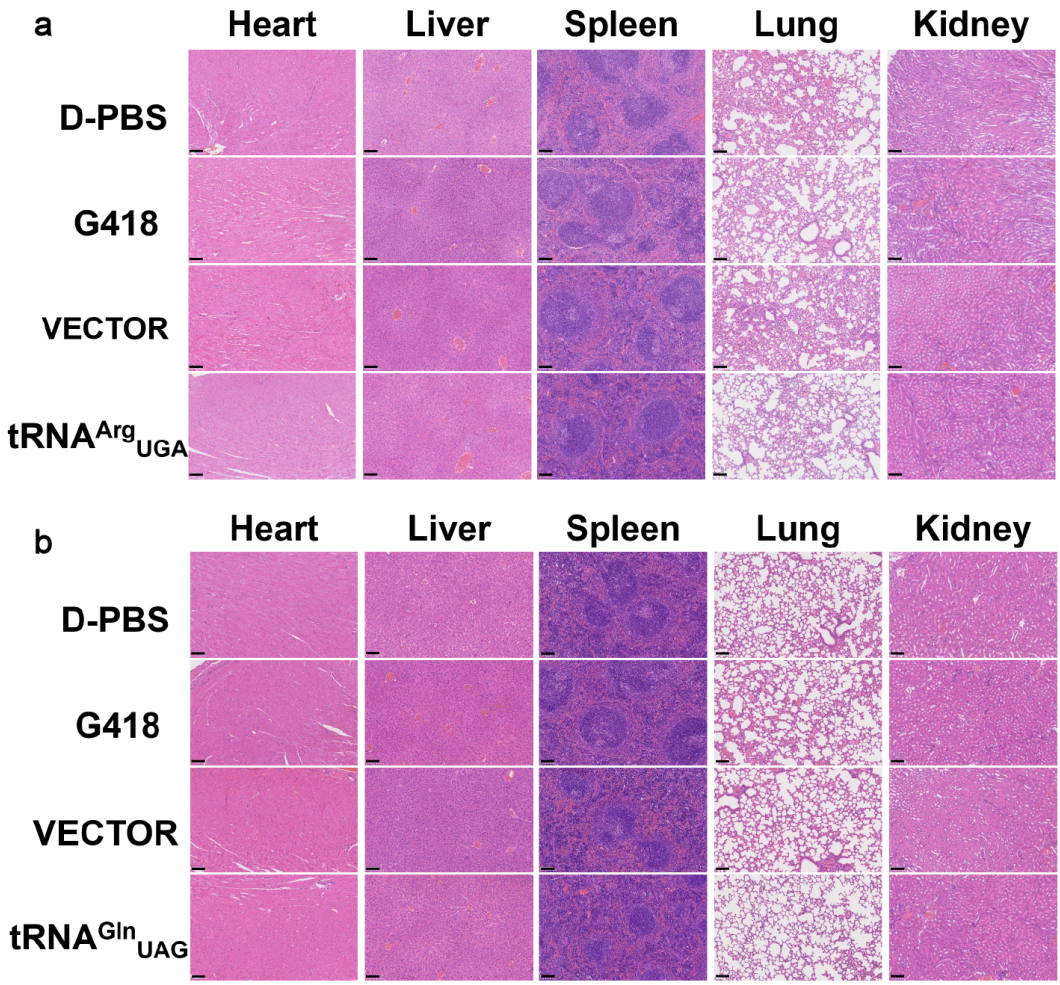


Supplementary Fig. 12 Characterization of LNP-tRNA formulations.
a TEM images of LNP-tRNA$^{Arg}_{UGA}$, LNP-tRNA$^{Gln}_{UAG}$ and LNP-VECTOR. Scale bars = 200 nm. **b** Analysis of the zeta potential (left corner) and size distribution and of LNP-tRNA$^{Arg}_{UGA}$, LNP-tRNA$^{Gln}_{UAG}$ and LNP-VECTOR. Data are mean ± SEM of n=3 biological replicates. Source data are provided as a Source Data file.

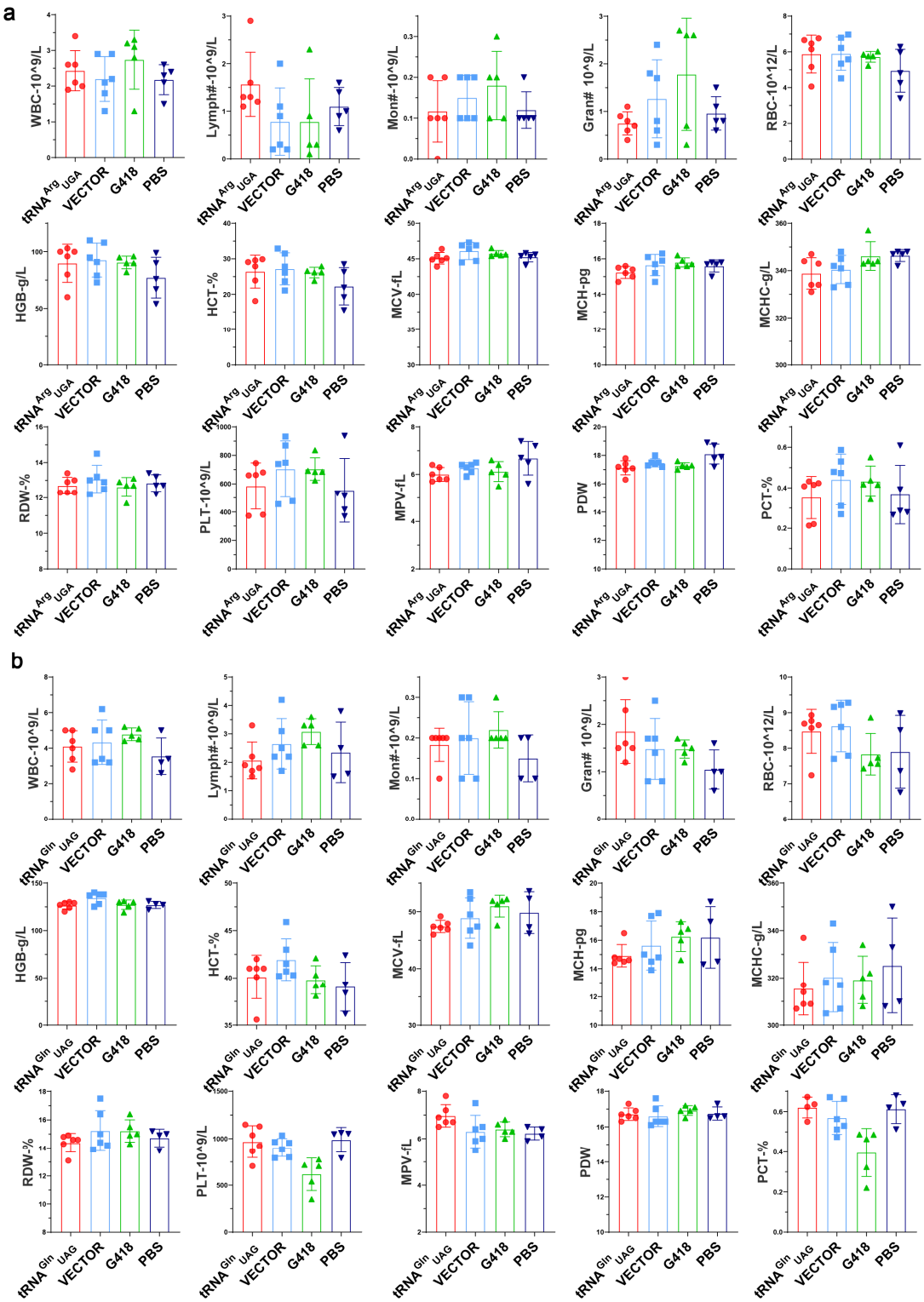


Supplementary Fig. 13 Body weight and survival curves of BALB/c nude after sup-tRNA treatment.

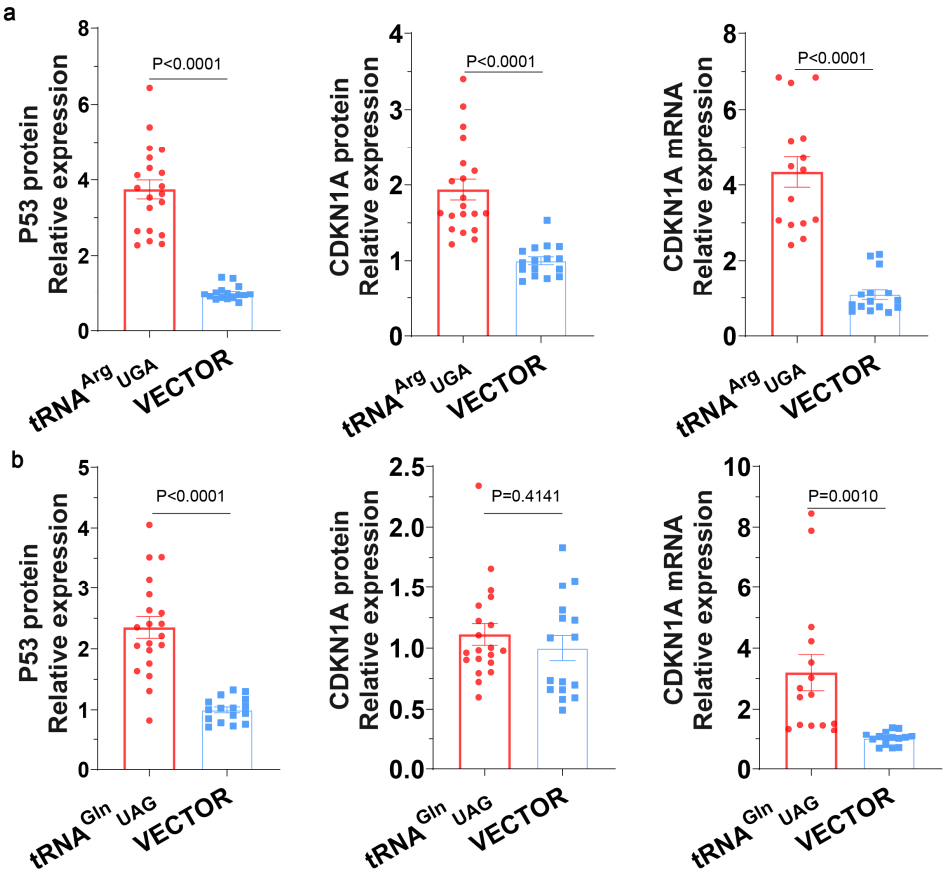
a, **b**, Body weight (**a**), and Kaplan-Meier survival curves (**b**) in Calu-6 xenograft model after LNP-tRNA$^{Arg}_{UGA}$ treatment. **c**, **d**, Body weight (**c**), and Kaplan-Meier survival curves (**d**) in Caco-2 xenograft model after LNP-tRNA$^{Gln}_{UAG}$ treatment. Data are presented as mean ± SEM. Source data are provided as a Source Data file.



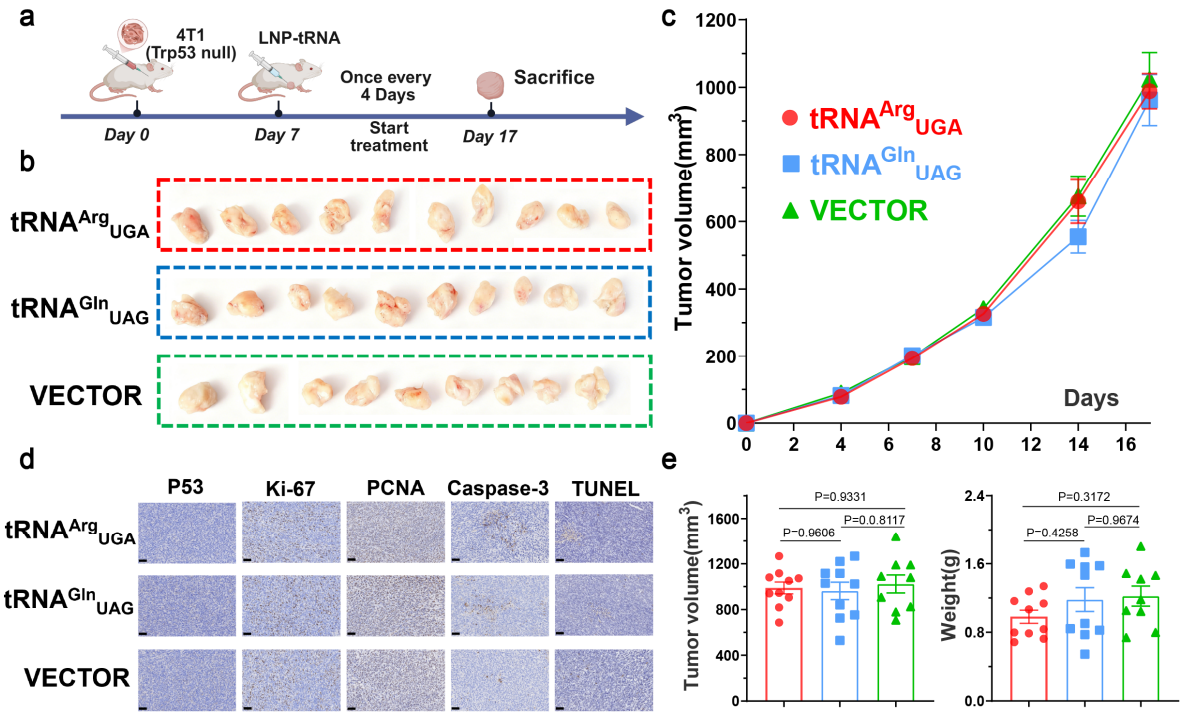
Supplementary Fig. 14 H&E staining of major organs after *in vivo* sup-tRNA treatment. **a**, **b** H&E staining of heart, liver, spleen, lung and kidney from Calu-6 (**a**) and Caco-2 (**b**) xenograft nude mice treated with sup-tRNAs. Scale bars = 100 μm. Data shown here were representative examples from n = 3 biological replicates.



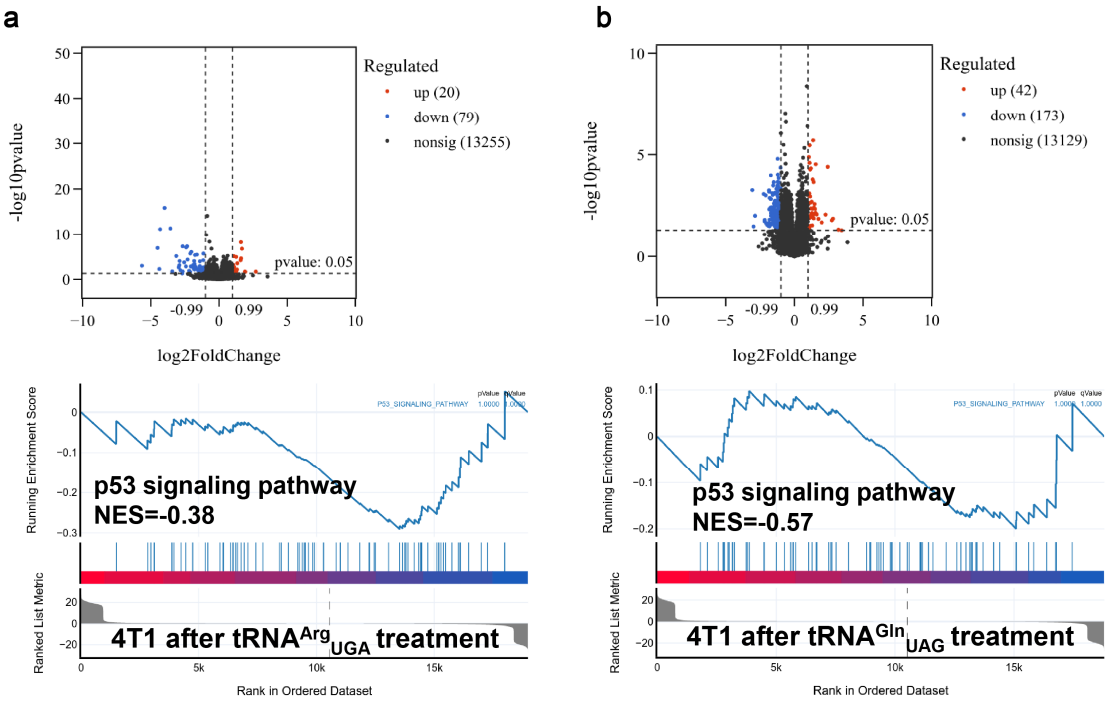
Supplementary Fig. 15 Blood examination after i*n vivo* sup-tRNA treatment.
a, **b** Complete blood count (CBC) analysis of Calu-6 (**a**) and Caco-2 (**b**) xenograft nude mice after sup-tRNAs treatment. Data are mean ± SEM of at least four biological replicates. Source data are provided as a Source Data file.



Supplementary Fig. 16 Protein and mRNA expression analysis after *in vivo* sup-tRNA treatment.
a p53 (left) & CDKN1A protein (middle) and CDKN1A mRNA (right) expression in Calu-6 xenograft treated with $tRNA^{Arg}_{UGA}$. Data are mean ± SEM of n=3 biological replicates. P-values were calculated by two-tailed student's t-test. **b** p53 (left) & CDKN1A protein (middle) and CDKN1A mRNA (right) expression in Caco-2 xenograft treated with $tRNA^{Gln}_{UAG}$. Data are mean ± SEM of n=3 biological replicates. P-values were calculated by unpaired two-tailed t-test. Source data are provided as a Source Data file.

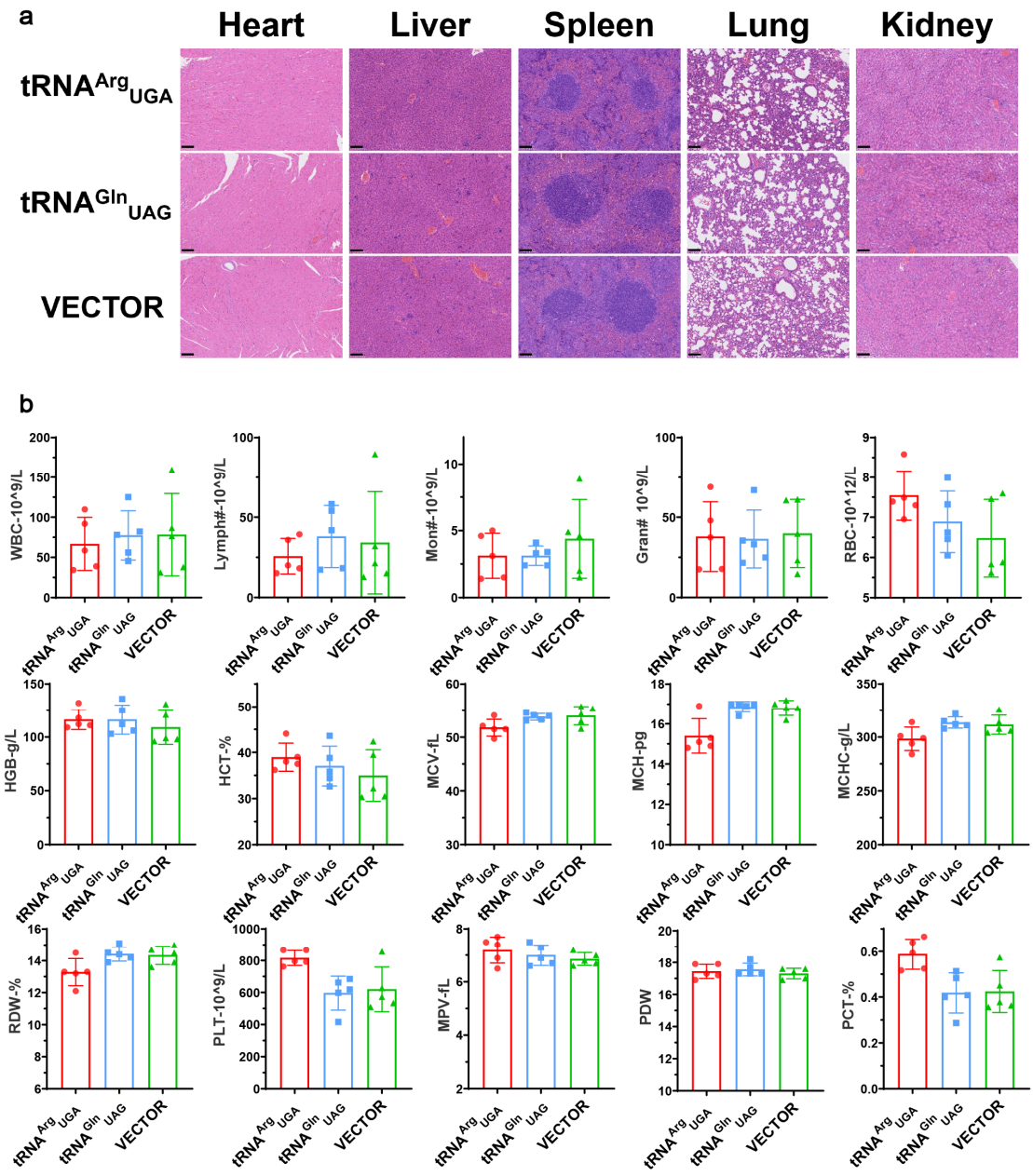


Supplementary Fig. 17 Evaluation of sup-tRNA in 4T1(*Trp53*-null) syngeneic tumour model. **a** Schematic of therapeutic evaluation of sup-tRNA therapy in 4T1 syngeneic tumour model. Created in BioRender. Chen, H. (2026) https://BioRender.com/8n41tem. **b** Images of 4T1 excised tumours. **c** Tumour growth curves of 4T1 syngeneic tumour model after sup-tRNA treatment (n = 10 mice in tRNA groups, n = 9 mice in VECTOR group). **d** Immunohistochemistry analysis of 4T1 tumour including p53, proliferation and apoptosis markers after corresponding treatments. Scale bar = 50 μm. Data shown here were representative examples from n = 3 independent biological replicates. **e** Tumour volumes (left) and weights(right) at endpoint (n = 10 mice in tRNA groups, n = 9 mice in VECTOR group). P-values were calculated by one-way ANOVA with Dunnett's correlation. Data are presented as mean ± SEM. Source data are provided as a Source Data file.



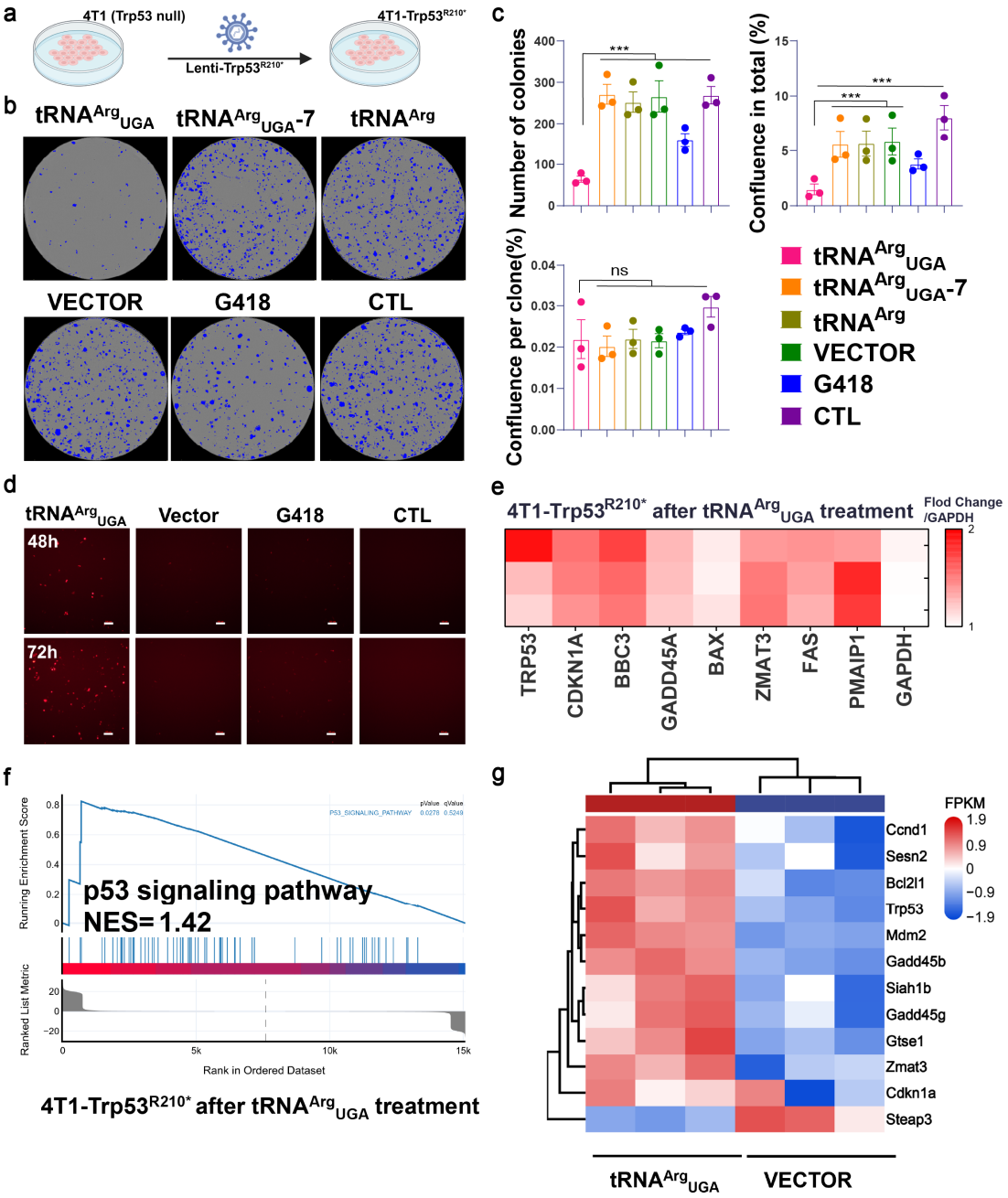
Supplementary Fig. 18 RNA-seq analysis of sup-tRNA in 4T1*(Trp53*-null*)* syngeneic tumour model.

a, **b**, Gene expression analysis (above) and Gene Set Enrichment Analysis (GSEA) of p53 signaling pathways (below) of 4T1 treated with tRNA$^{Arg}_{UGA}$ (**a**) and tRNA$^{Gln}_{UAG}$ (**b**) *in vivo*. N=3 biological replicates.



Supplementary Fig. 19 Safety evaluation of sup-tRNA in mice bearing syngeneic 4T1 tumours.

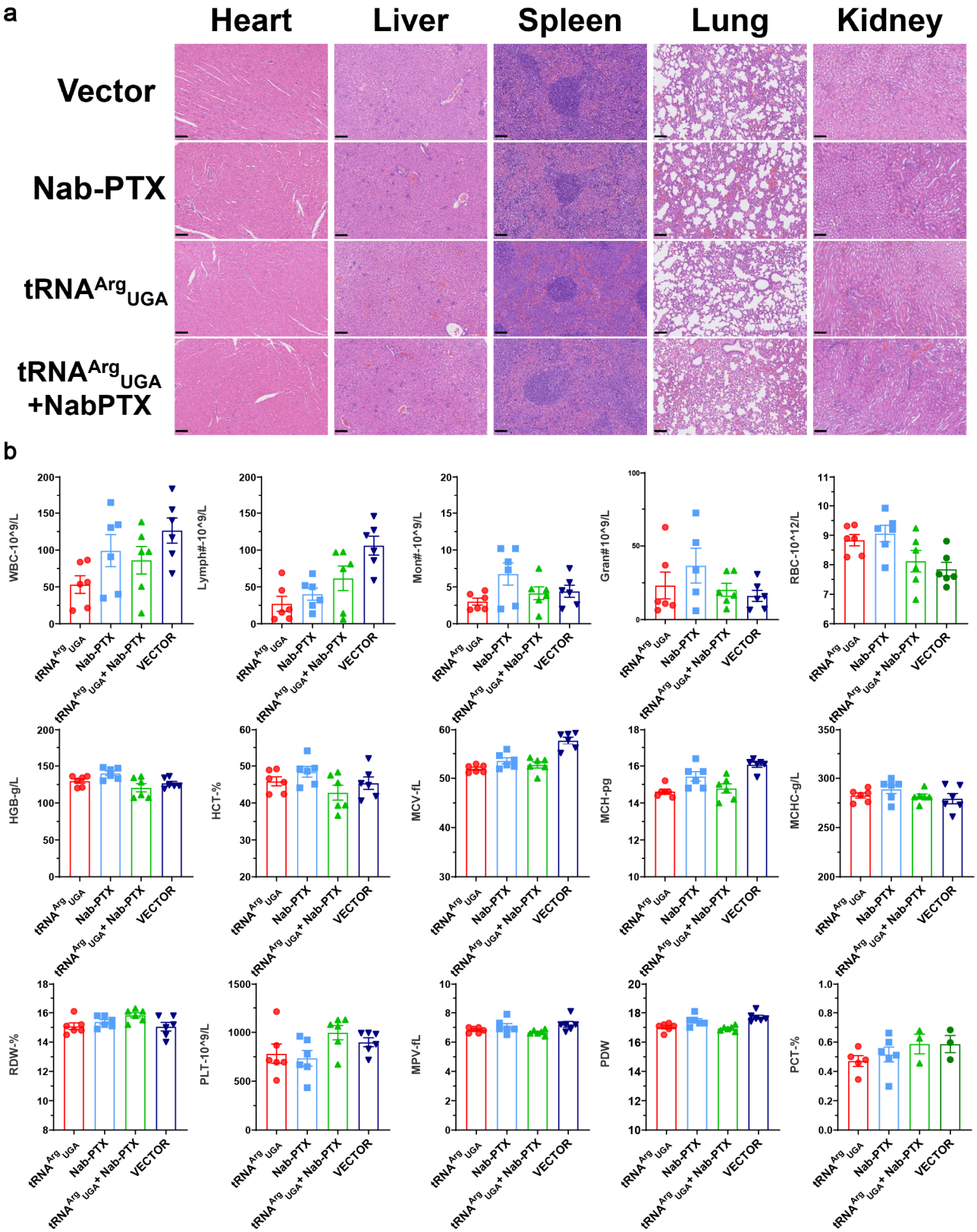
a H&E staining of heart, liver, spleen, lung and kidney of mice bearing syngeneic 4T1 tumours after sup-tRNA treatment. Scale bars = 100 μm. Data shown here were representative examples from n = 3 biological replicates. **b** Complete blood count analysis of mice bearing syngeneic 4T1 tumours after sup-tRNA treatment. Data are mean ± SEM of at least four biological replicates. Source data are provided as a Source Data file.



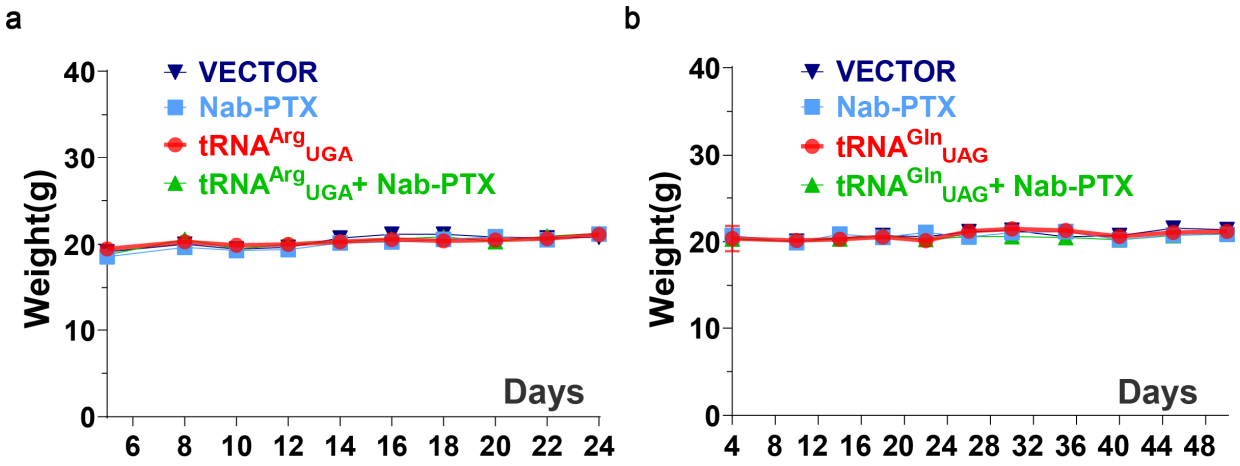
Supplementary Fig. 20 Sup-tRNA suppresses proliferation and restores p53 transcriptional activity in 4T1-*Trp53*^{R210*} cell line.

a Schematic workflow of 4T1-*Trp53*^{R210*} cell line construction. Created in BioRender. Chen, H. (2026) https://BioRender.com/v1fcw0y. **b**, **c**, Sup-tRNAs reduces the colony formation in 4T1-*Trp53*^{R210*} cells. Colonies are stained with crystal violet staining solution and counted after 10-12 days of culture. Colony images are acquired by Incucyte SX5 and processed and analyzed by Incucyte 2022B Rev2. Data are represented as mean ± SEM, n = 3 biological replicates. **d** Representative microscopy images showing the transcriptional activity of Trp53 in 4T1-*Trp53*^{R210*} cells treated with sup-tRNA, vector, and G418 for 48&72 hours. Data shown here were representative examples from n = 3 biological replicates. **e** Heatmap of mRNA expression levels of *Trp53* and its target genes *Cdkn1a*, *Bbc3*, *Gadd45a*, *Bax*, *Zmat3*, *Fas*, and *Pmaip1* after sup-tRNA

treatment in 4T1-*Trp53*^{R210*} cells for 48h by qRT-PCR. All the mRNA expression levels are normalized to *GAPDH*. Data are represented as mean for n = 3 biological replicates. Each cell in the heatmap (**e**) shows the result of one of n = 3 biological replicates. **f**, **g**, Gene Set Enrichment Analysis (**f**) and gene expression analysis (**g**) of p53 signaling pathways on 4T1-*Trp53*^{R210*} cells treated with sup-tRNA, or vector control, n = 3 biological replicates. *P < 0.05, **P < 0.01, ***P < 0.001, NS, not significant. Source data are provided as a Source Data file.

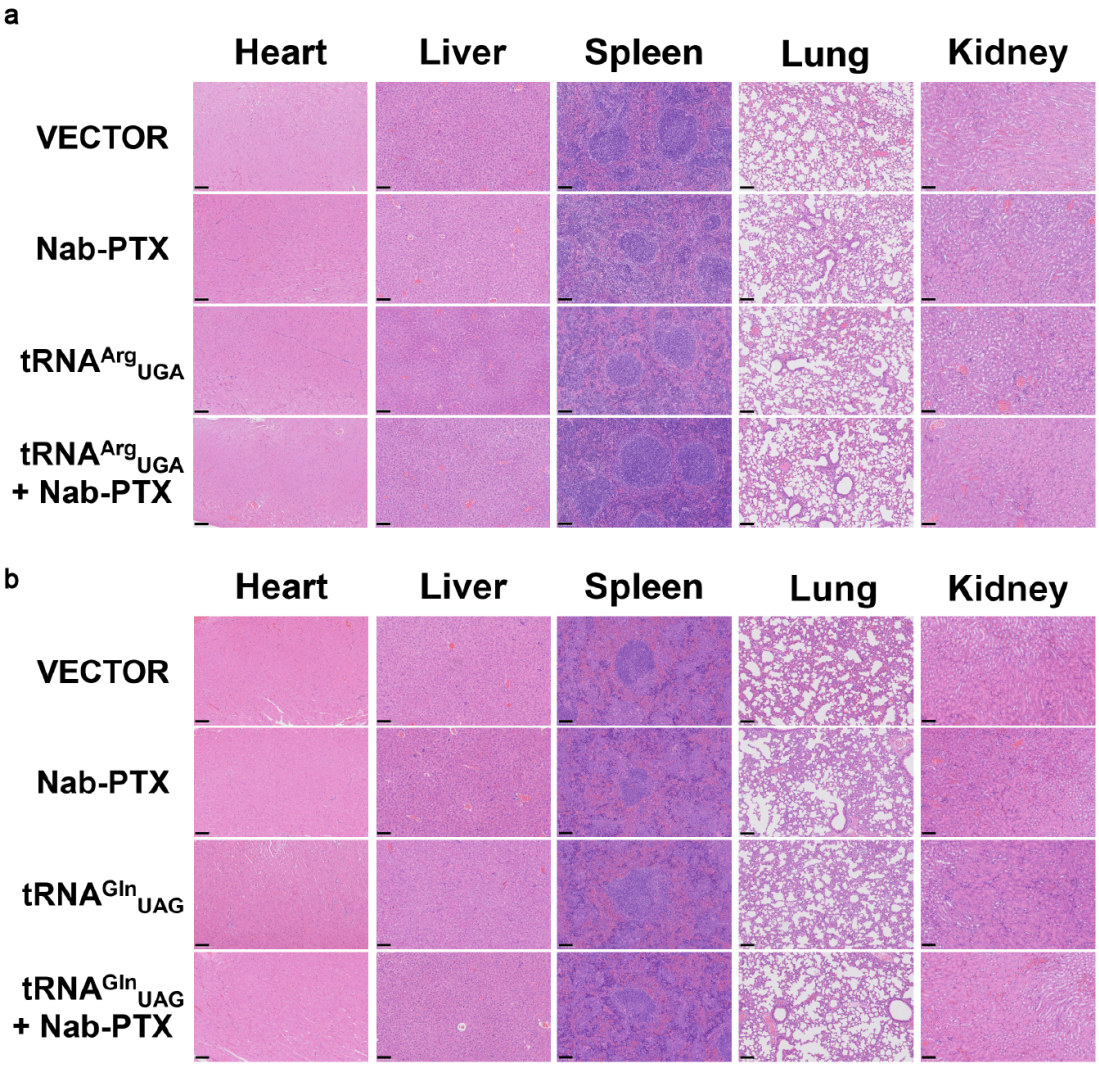

a
Heart
Liver
Spleen
Lung
Kidney
Vector
Nab-PTX
tRNA^Arg_UGA
tRNA^Arg_UGA +NabPTX
b
WBC-10^9/L
Lymph#-10^9/L
Mon#-10^9/L
Gran#10^9/L
RBC-10^12/L
HGB-g/L
HCT-%
MCV-fL
MCH-pg
MCHC-g/L
RDW-%
PLT-10^9/L
MPV-fL
PDW
PCT-%
tRNA^Arg_UGA
Nab-PTX
tRNA^Arg_UGA + Nab-PTX
VECTOR

Supplementary Fig. 21 Safety evaluation of sup-tRNA in mice bearing syngeneic 4T1-*Trp53*^{R210*} tumours.
a H&E staining of heart, liver, spleen, lung and kidney from mice bearing syngeneic 4T1-*Trp53*^{R210*} tumours after sup-tRNA treatment. Scale bars = 100 μm. Data shown here were representative examples from n = 3 biological replicates. **b** Complete blood count (CBC) analysis of mice bearing syngeneic 4T1-*Trp53*^{R210*} tumours after sup-tRNA treatment. Data are mean ± SEM of at least four biological replicates. Source data are provided as a Source Data file.



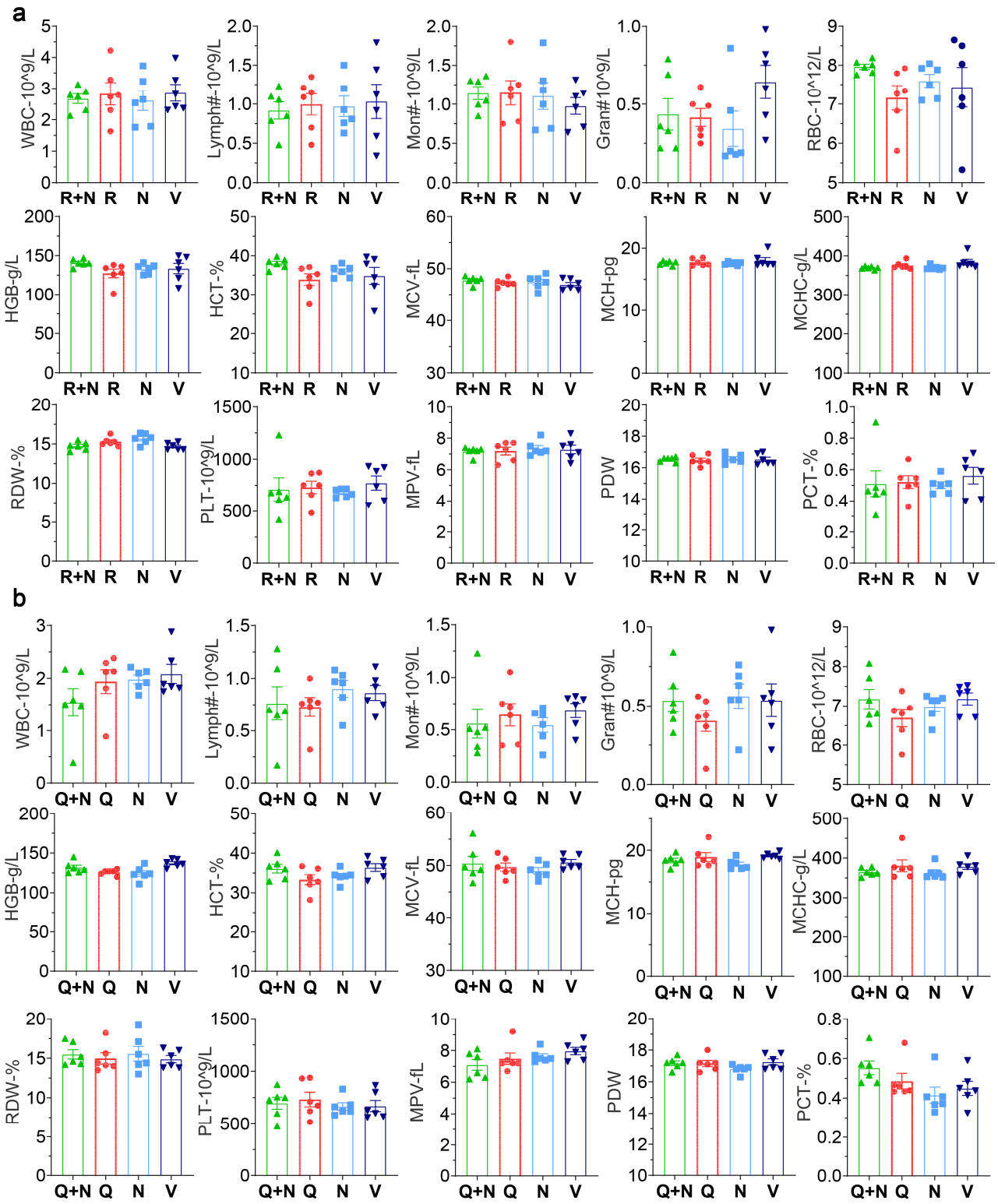
Supplementary Fig. 22 Body weights of BALB/c nude after sup-tRNAs, Nab-PTX, or their combination treatment.

a, **b** Body weight curve of Calu-6 (**a**) and Caco-2 (**b**) xenograft model after sup-tRNAs, Nab-PTX, or their combination treatment. Data are presented as mean ± SEM. Source data are provided as a Source Data file.



Supplementary Fig. 23 H&E staining of major organs after sup-tRNAs, Nab-PTX, or their combination treatment.

a, **b** H&E staining of heart, liver, spleen, lung and kidney from Calu-6 (**a**) and Caco-2 (**b**) xenograft nude mice treated with sup-tRNAs, Nab-PTX, or their combination, assessed by H&E staining. Scale bars = 100 μm. Data shown here were representative examples from n = 3 biological replicates.



Supplementary Fig. 24 Blood examination after sup-tRNAs, Nab-PTX, or their combination *in vivo* treatment.

a, **b** Complete blood count (CBC) analysis of Calu-6 (**a**) and Caco-2 (**b**) xenograft nude mice, treated with sup-tRNA, Nab PTX or their combination. Data are mean ± SEM of at least four biological replicates. The abbreviation for $tRNA^{Arg}_{UGA}$ is R, the abbreviation for $tRNA^{Gln}_{UAG}$ is Q, the abbreviation for Nab-PTX is N and the abbreviation for VECTOR is V. Source data are provided as a Source Data file.

Supplementary Table 1. Identification and analysis of driver TSG mutations

Dependent variables	(1) Cancer types where is driver	(2) Cohorts where is driver	(3) Cancer types where is driver	(4) Cohorts where is driver	(5) Cancer types where is driver	(6) Cohorts where is driver
Nonsense_COSMIC	0.586***	1.451***				
	(5.36)	(5.12)				
Missense_COSMIC			0.039	0.097		
			(1.11)	(0.93)		
Synonymous_COSMIC					-0.222***	-0.685***
					(-2.68)	(-2.81)
Constant	0.881*	-1.191	2.924**	3.840	7.189***	16.054***
	(1.68)	(-0.93)	(2.21)	(1.00)	(5.96)	(4.37)
Observations	314	314	314	314	314	314
R-squared	0.250	0.228	0.005	0.005	0.036	0.050

Dependent variables	(1) Cancer types where is driver	(2) Cohorts where is driver	(3) Cancer types where is driver	(4) Cohorts where is driver	(5) Cancer types where is driver	(6) Cohorts where is driver
Truncating _IntOGen	0.237***	0.614***				
	(5.47)	(5.38)				
Missense_IntOGen			-0.236***	-0.570***		
			(-4.13)	(-3.74)		
Synonymous_IntOGen					-0.375***	-1.052***
					(-4.34)	(-3.76)
Constant	0.643	-2.241	18.923***	42.622***	12.206***	29.407***
	(1.14)	(-1.63)	(5.25)	(4.49)	(6.07)	(4.54)
Observations	314	314	314	314	314	314
R-squared	0.187	0.187	0.104	0.091	0.147	0.173

Robust t-statistics in parentheses

Ordinary least squares (OLS) linear regression analysis between the proportion of mutation types of TSGs and their driver ability. Robust t-statistics are in parentheses. Nonsense/truncation mutations data is derived from IntOGen & COSMIC, and the number of driver cancer types and cohorts is derived from IntOGen. *P < 0.05, **P < 0.01, ***P < 0.001, NS, not significant.

Supplementary Table 2. qPCR primers

For human genes：

Gene	Primer type	sequence：5'- 3'
GAPDH (*Homo sapiens)*	Forward primer	5′- GGAGCGAGATCCCTCCAAAAT-3′
	Reverse primer	5′- GGCTGTTGTCATACTTCTCATGG-3′
TP53 (*Homo sapiens*)	Forward primer	5′- CAGCACATGACGGAGGTTGT-3′
	Reverse primer	5′- TCATCCAAATACTCCACACGC -3′
CDKN1A (*Homo sapiens*)	Forward primer	5′- TGTCCGTCAGAACCCATGC -3′
	Reverse primer	5′- AAAGTCGAAGTTCCATCGCTC -3′
BBC3 (*Homo sapiens*)	Forward primer	5′- GCCAGATTTGTGAGACAAGAGG -3′
	Reverse primer	5′- CAGGCACCTAATTGGGCTC -3′
GADD45A (*Homo sapiens*)	Forward primer	5′- GAGAGCAGAAGACCGAAAGGA -3′
	Reverse primer	5′- CACAACACCACGTTATCGGG -3′
BAX (*Homo sapiens*)	Forward primer	5′- CCCGAGAGGTCTTTTTCCGAG -3′
	Reverse primer	5′- CCAGCCCATGATGGTTCTGAT -3′
ZMAT3 (*Homo sapiens*)	Forward primer	5′- AGAAGCCTTTTGGGCAGGAG -3′
	Reverse primer	5′- TGCTGCATAGTAATTTCGGAGTT -3′
FAS (*Homo sapiens*)	Forward primer	5′- TCTGGTTCTTACGTCTGTTGC -3′
	Reverse primer	5′- CTGTGCAGTCCCTAGCTTTCC -3′
PMAIP1 (*Homo sapiens*)	Forward primer	5′- ACCAAGCCGGATTTGCGATT -3′
	Reverse primer	5′- ACTTGCACTTGTTCCTCGTGG -3′

For mouse genes：

Gene	Primer type	sequence：5’- 3’
GAPDH (*Homo sapiens)*	Forward primer	5′- GGAGCGAGATCCCTCCAAAAT-3′
	Reverse primer	5′-GGCTGTTGTCATACTTCTCATGG-3′
TP53 (*Homo sapiens*)	Forward primer	5′- CAGCACATGACGGAGGTTGT -3′
	Reverse primer	5′- TCATCCAAATACTCCACACGC -3′
CDKN1A (*Homo sapiens*)	Forward primer	5′- TGTCCGTCAGAACCCATGC -3′
	Reverse primer	5′- AAAGTCGAAGTTCCATCGCTC -3′
Gapdh (*Mus musculus)*	Forward primer	5′- AGGTCGGTGTGAACGGATTTG -3′
	Reverse primer	5′- GGGGTCGTTGATGGCAACA -3′
Trp53 (*Mus musculus*)	Forward primer	5′- CCCCTGTCATCTTTTGTCCCT -3′
	Reverse primer	5′- AGCTGGCAGAATAGCTTATTGAG -3′
Cdkn1a (*Mus musculus*	Forward primer	5′- CCTGGTGATGTCCGACCTG -3′
	Reverse primer	5′- CCATGAGCGCATCGCAATC -3′
Bbc3 (*Mus musculus*)	Forward primer	5′- AGCAGCACTTAGAGTCGCC -3′
	Reverse primer	5′- CCTGGGTAAGGGGAGGAGT -3′
Gadd45a (*Mus musculus*)	Forward primer	5′- AGACCGAAAGGATGGACACG -3′
	Reverse primer	5′- GTACACGCCGACCGTAATG -3′
Bax (*Mus musculus*)	Forward primer	5′- AGACAGGGGCCTTTTTGCTAC -3′
	Reverse primer	5′- AATTCGCCGGAGACACTCG -3′
Zmat3 (*Mus musculus*)	Forward primer	5′- TGGCTTCCTTTACCTAATCGGC -3′

	Reverse primer	5′- GGGGCTTACACAGCTCCTC -3′
Fas (*Mus musculus*)	Forward primer	5′- GCGGGTTCGTGAAACTGATAA -3′
	Reverse primer	5′- GCAAAATGGGCCTCCTTGATA -3′
Pmaip1 (*Mus musculus*)	Forward primer	5′- GCAGAGCTACCACCTGAGTTC -3′
	Reverse primer	5′- CTTTTGCGACTTCCCAGGCA -3′